Short-Range Ultrasonic Communications in Air Using Quadrature Modulation

Chuan Li, David A. Hutchins, and Roger J. Green, *Senior Member, IEEE*

***Abstract*—A study has been undertaken of ultrasonic communications methods in air, using a quadrature modulation method. Simulations were first performed to establish the likely performance of quadrature phase shift keying over the limited bandwidth available in an ultrasonic system. Quadrature phase shift keying modulation was then implemented within an experimental communication system, using capacitive ultrasonic sources and receivers. The results show that such a system is feasible in principle for communications over distances of several meters, using frequencies in the 200 to 400 kHz range.**

I. Introduction

In recent years, short-range wireless communications have been mostly dominated by RF systems [1] using a wide variety of technologies, including popular commercial protocols such as IEEE802 [2], and Bluetooth [3], among others. Here, a short range is usually defined as 10 to 50 m indoors and 50 to 200 m outdoors, although propagation over longer ranges is possible. Another technique for short range use is infrared communication [4] using protocols such as IrDA [5]. The data rate in such communication systems typically ranges from kilobits per second to gigabits per second. These methods are successful and in widespread use. However, other types of signals by which information can be communicated over short distances may have an advantage in certain situations. One such consideration is security [6]. For instance, RF signals are easy to intercept and various forms of encoding are needed to maintain secure data transfer [7]. Infrared technology is, in principle, more secure for short-range use, but can suffer from daylight and artificial light interference. Nevertheless, its output power is strictly limited by eye safety regulations.

An alternative approach is to consider the use of ultrasound in air for communications. This offers several advantages over existing methods, especially for security—it is effectively blocked by most barriers and has a limited propagation range, making interception from outside a room very difficult. It also has other beneficial qualities. For instance, the slow propagation speed in air allows the location of sources to be tracked. In addition, problems caused by multi-path effects (interference from direct and reflected signals [8]) can potentially be reduced, because of the difference in propagation time for multiple paths. Despite these attractive qualities, development of ultrasonic short-range communication systems has been somewhat restricted, because of the narrow bandwidth of available acoustic transducers and the high attenuation of ultrasound propagation in air at frequencies above 2 MHz. However, with recent developments in transducer technology for use in air, including wide bandwidth capacitive [9] and piezoelectric [10] designs, the effective operating bandwidth now stretches to 1 MHz and beyond. As a result, reasonable data rates of up to several hundred kilobits per second can be expected, provided suitable modulation data recovery methods are developed.

Initial studies of the properties of ultrasonic communication systems have been published. For instance, a wireless keyboard using ultrasound has been designed [11]. Recently, ultrasound has been used for location tracking in hospitals, where time-of-flight from a moving source to a set of fixed receivers can be used [12]. Other work has looked at simple methods for designing an ultrasonic PC mouse [13] using narrow bandwidth piezoelectric transducers with a center frequency of 40 kHz in an analog modulation scheme. An ultrasonic communication system has also been developed where data (for example, characters, images, and voice) could be sent ultrasonically through air or pipes with or without water, using commercially available piezoelectric transducers at a data rate of 100 bits per second [14]. For data transmission in air, another study compared digital modulation techniques based on binary phase shift keying (BPSK) and binary frequency shift keying (BFSK), 2 common forms of modulation. This demonstrated that signals could be transmitted in air over a 3-m distance at a data rate of 5 kb/s [15], with BPSK being the better of the 2 types of digital modulation.

There are, however, more advanced methods of modulation available which can be used in short-range air-coupled ultrasonic systems. These are so-called quadrature methods. Quadrature phase modulation has been successfully adapted to underwater ultrasonic communications [16], where data was sent at a transmission rate of 80 kb/s over a distance of 350 m underwater. One of the most widely-used variants is quadrature phase shift keying (QPSK). In general, the main advantage of QPSK is that it can reach a data rate twice that of BPSK, while preserving similar levels of bit error rate (BER), which is a measure of how accurately the data are being transmitted. By using raised cosine (RC) pulse shaping, the required bandwidth could be further reduced.

The motivation for the work described in this paper was to characterize the performance of QPSK when operating over a bandwidth-limited ultrasonic communication channel in air. The next section provides some background

Manuscript received December 9, 2008; accepted June 5, 2009.

The authors are with the School of Engineering, University of Warwick, Coventry, UK (e-mail: chuan.li@warwick.ac.uk).

Digital Object Identifier 10.1109/TUFFC.2009.1289

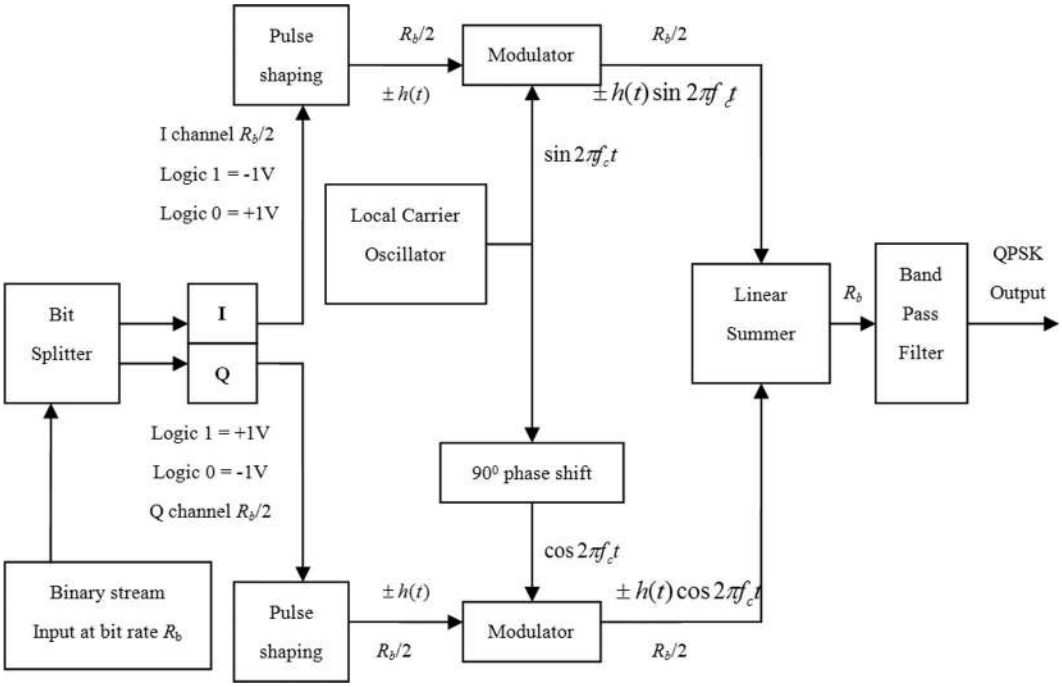

Fig. 1. Schematic diagram of a quadrature phase shift keying (QPSK) modulator.

about QPSK modulation and methods of pulse shaping. This is followed by a numerical simulation of such an approach, together with apparatus and results from experiments with capacitive transducers.

II. Quadrature Phase Shift Keying for Data Communications

It is informative to first describe the main features of QPSK, the approach being considered for ultrasonic communications. QPSK, sometimes also referred to as quaternary phase shift keying, is a form of angle-modulated, constant-amplitude digital modulation. It consists of 4 different output phases (0, $\pi/2$, π, and $3\pi/2$), based on 4 different binary signal input conditions (00, 01, 11, 10). Because each cycle of the carrier contains 2 bits of information, the bandwidth of the output signal is half what it would have been if quadrature methods had not been used. There is thus an increase in bandwidth efficiency over non-quadrature methods.

A block of diagram of a QPSK modulator used to generate a suitable transmission digital waveform (the QPSK output), is shown in Fig. 1. The binary stream to be transmitted at a bit rate of R_b is input as a serial binary stream into a bit splitter. This creates 2 simultaneously parallel channels, namely the in-phase channel (**I**), and the quaternary-phase channel (**Q**) which is 90° out of phase with **I**. For a logic 1 = +1 V and logic 0 = −1V, 2 phases are possible at the output of the **I** modulator, and 2 phases are possible at the output of the **Q** modulator. When the 2 quadrature signals are finally added at the linear summer stage, there are 4 possible resultant phasors, given by the following expression:

TABLE I. Truth Table for Quadrature Phase Shift Keying (QPSK) Modulation.

Binary input		QPSK output phase
I	Q	
0	0	+45
0	1	+135
1	1	−135
1	0	−45

$$\pm \sin 2\pi f_c t \pm \cos 2\pi f_c t, \tag{1}$$

where f_c is the carrier frequency in hertz and t is time in seconds. The truth table for QPSK is shown in Table I, with the diagram of Fig. 2 indicating that the angular separation between any 2 adjacent phasors in QPSK is 90°. Therefore, a QPSK signal can undergo almost a +45° or −45° shift in phase during transmission and still retain the correct encoded information when demodulated at the receiver.

The bandwidth B of a QPSK signal can be expressed as

$$B = \left(f_c + \frac{f_b}{4}\right) - \left(f_c - \frac{f_b}{4}\right) = \frac{f_b}{2}, \tag{2}$$

where f_b is equivalent to the bit rate R_b in hertz. Mathematically, QPSK signals can be defined as

$$S_{\text{QPSK}}(t) = A\cos\left[\omega_c t + (i-1)\frac{\pi}{2}\right] \quad 0 \le t \le T_s, i = 1,2,3,4, \tag{3}$$

where signal amplitude A in volts can be represented as

$$A = \sqrt{\frac{2E_s}{T_s}}, \tag{4}$$

and angular frequency ω_c in radians can be defined as

$$\omega_c = 2\pi f_c. \tag{5}$$

Here, T_s is the symbol duration in seconds and is equal to twice the bit duration. E_s is the symbol energy in joules, f_c is the carrier frequency, and i is the symbol number. By using trigonometric identities, the above equations can be rewritten as

$$S_{\text{QPSK}} = A\cos\left[(i-1)\frac{\pi}{2}\right]\cos(\omega_c t) - A\sin\left[(i-1)\frac{\pi}{2}\right]\sin(\omega_c t). \tag{6}$$

The first term in (6) represents the in-phase channel, and the second term is the quadrature phase channel. The average probability of bit error in the additive white Gaussian noise (AWGN) channel is obtained as

$$P_{e,\text{QPSK}} = \frac{1}{2}\text{erfc}\left(\sqrt{\frac{E_b}{N_0}}\right), \tag{7}$$

where E_b/N_0 is the energy per bit to noise spectral density ratio. The complementary error function, denoted erfc, is defined as

$$\text{erfc}(x) = \frac{2}{\sqrt{\pi}}\int_x^\infty e^{-x^2}dt. \tag{8}$$

Coherent detection [16] is often used for demodulation, and for this it is essential to have an effective local carrier frequency in phase with the original carrier frequency used for transmission. A typical QPSK demodulator is shown in Fig. 3. The received QPSK signal, after being bandpassed to reject any noise, is passed through 2 product modulators simultaneously, with the I-channel multiplied by the synchronized carrier and the Q-channel multiplied by a 90° phase shift carrier. The products are then passed through 2 low-pass filters to recover the I-channel and Q-channel baseband signals. Finally, a threshold detector is used to form the decoded binary stream. If the amplitude of the signal is greater than 0 V at the sampling point, a logic '1' is decoded; if smaller than 0 V, a logic '0' is recovered.

Pulse shaping is normally used to reduce inter-symbol interference (ISI), which usually caused by multipath propagation and the inherent nonlinear frequency response of a channel. Raised cosine shaping of the transmitted bits baseband spectrum is one of the best filter forms to reduce ISI as well as the bandwidth of the signal. Its transfer function can be represented as

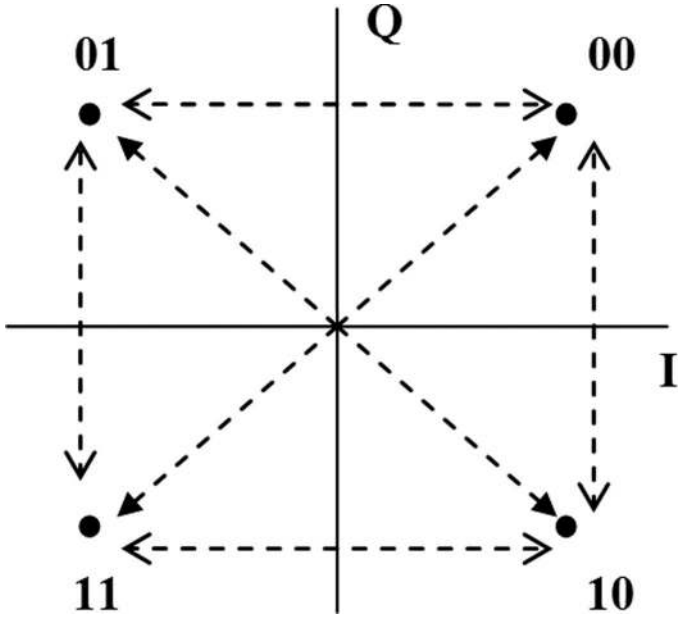

Fig. 2. Constellation diagram for quadrature phase shift keying modulation. Q = quaternary-phase channel; I = in-phase channel.

$$H_{\text{RC}}(f)\begin{cases}1 & 0 \le |f| \le \frac{(1-\alpha)}{2T_s} \\ \frac{1}{2}\left[1+\cos\left[\frac{\pi(|f|\cdot 2T_s - 1+\alpha)}{2\alpha}\right]\right] & \frac{(1-\alpha)}{2T_s} \le |f| \le \frac{(1+\alpha)}{2T_s} \\ 0 & |f| > \frac{(1+\alpha)}{2T_s}.\end{cases} \tag{9}$$

Here, α is the roll-off factor, which ranges between 0 and 1. When $\alpha = 0$, the raised cosine roll-off filter corresponds to a rectangular filter of minimum bandwidth. As the roll-off factor α increases, the bandwidth B of the filter also increases, according to

$$R_s = \frac{B}{1+\alpha}, \tag{10}$$

where R_s is the symbol rate in symbols per seconds, and B is absolute filter bandwidth.

There are various factors which are important in a particular modulation scheme and which help to measure its performance. The error vector magnitude (EVM) is one such factor. This is the magnitude of the vector drawn between the ideal symbol position of the constellation, or hard decision, and the measured symbol position, or soft decision. It is mathematically given by

$$\text{EVM} = \frac{E_{\text{RMS}}}{S_{\max}} \times 100\% \tag{11}$$

where (E_{RMS}) is the RMS error magnitude, and $S_{\max}$ is the maximum received symbol magnitude. The lower the EVM is, the better the performance of the system. Another measure is the modulation error ratio (MER) which

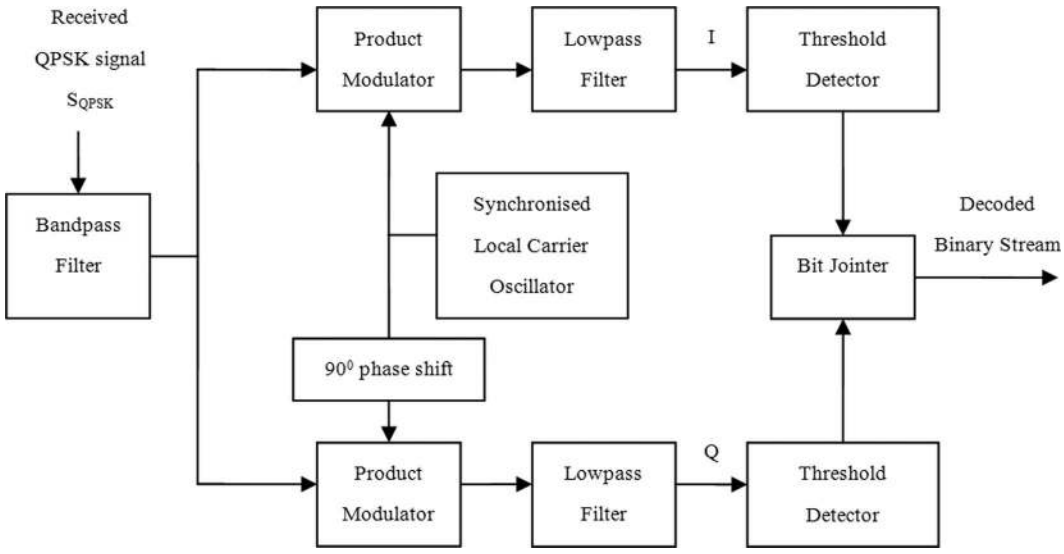

Fig. 3. Schematic diagram of a quadrature phase shift keying (QPSK) demodulator.

is a form of SNR for a complex digital baseband. In fact, the terms SNR and MER are often used interchangeably. They are direct measures of modulation quality. MER is defined as the ratio of the average symbol power to the average error power, and is normally expressed in decibels, as follows:

$$\mathrm{MER(dB)} = 10\log_{10}\left[\frac{\sum_{j=1}^{N}(I_j^2 + Q_j^2)}{\sum_{j=1}^{N}(\delta I_j^2 + \delta Q_j^2)}\right]. \qquad (12)$$

Here, I_j and Q_j are the real (in-phase) and imaginary (quadrature) parts of each sampled ideal target symbol vector, and δI and δQ are the real (in-phase) and imaginary (quadrature) parts of each modulation error vector. In effect, MER is a measure of how fuzzy the symbol points of a constellation are. Ideally, MER should have a value as high as possible.

In estimating the performance of such communication systems, the channel capacity (C), measured in bits per second, is an important parameter, because it defines the information-carrying capacity of a given communication channel. The most widely used estimate is given by Shannon's channel capacity formula [17], which is given by

$$C = B\log_2\left(1 + \frac{E_b R_b}{N_0 B}\right) = B\log(1 + \mathrm{SNR}). \qquad (13)$$

Here, E_b is the signal energy in joules per bit, R_b is the transmission bit rate in bits per second, which is twice the symbol rate R_s for quadrature phase modulation. N_0 is the signal noise power spectral density, expressed in watts/hertz, within the bandwidth B. The ratio E_b/N_0 can be used to calculate the value of SNR that must be present to achieve a given bit rate R_b for a given known channel capacity C. The maximum bandwidth efficiency is given by the ratio C/B.

III. Apparatus and Experiment

The previously described quadrature methods have been investigated experimentally for an ultrasonic communication system using capacitive transducers for use in air. These devices, which have been described elsewhere [18], [19], have been designed to give an ultrasonic response that extends up to 2 MHz. Their broad bandwidth and excellent sensitivity make them ideal for air-based communication systems [11], and arise from careful design of a flexible polymer membrane in conjunction with a rigid, machined backplate.

As shown in Fig. 4, these devices are composed of a thin metalized membrane film and a rigid contoured, conducting backplate to form a capacitor. Applied voltages cause the membrane to vibrate, and hence generate ultrasound, whereas ultrasound impinging on the membrane changes the device's capacitance, allowing it to be used for detection. This type of transducer was found to be very sensitive at high bias voltages when a thin polymer membrane was used. In addition, these small etched air pits help to trap air beneath the membrane and reduce the membrane rigidity and thus produce a wider bandwidth and enhanced sensitivities.

Fig. 5 shows a typical experimental arrangement, where the transmitter and receiver are placed at a distance of 1.2 m. The transmitter has a membrane thickness of 5 μm, so as to withstand higher excitation voltages without causing damage to the polymer membrane. The source was driven by an Agilent 33120A arbitrary waveform generator (Agilent Technologies, Inc., Santa Clara, CA), with a superimposed +100 V dc bias voltage generated by a dc power supply. This supplied the required digital signal for transmission. A linear power amplifier with a gain of 25 dB was used to boost the output of the waveform generator. The receiver had a film thickness of 2.5 μm and was followed by a Cooknell CA6/C charge amplifier (Cooknell Electronics Ltd., Dorest, UK)

with a gain of 250 mV/pC. The response was then fed into a Tektronix TDS210 digital oscilloscope (Tektronix, Inc., Beaverton, OR) for signal analysis. Finally, the waveforms were saved on a PC running Labview 7.2 (National Instruments, Austin, TX) for offline signal processing. A physical synchronization link was established between the waveform generator and the oscilloscope. This removed the need for wireless handshaking, which would be needed in a real application.

Note that the output signal amplitude was typically set at 200 V peak-to-peak after amplification, and the received signal amplitude was typically around 5 mV rms at 1.2 m. The experiment was performed in an indoor laboratory where room temperature was about 25°C and the relative humidity was around 79%. The recorded background noise level was around 600 μV rms, with negligible air turbulence to influence the signal transmission.

The measured overall response of the communication channel (in terms of amplitude and phase) was required for the simulations of the quadrature approach which appear in the next section of this paper. As shown in Fig. 6(a), the magnitude response peaks at 300 kHz, but has a dip at 880 kHz. The 6-dB bandwidth of the measured channel is about 350 kHz, and the usable frequency range is about 900 kHz. Fig. 6(b) shows that the phase response of the channel is roughly linear across the 6-dB bandwidth.

IV. Numerical Simulations

Simulations were undertaken, using the experimental response found in Section III, to determine the expected performance of various RC-shaped QPSK signals and the unshaped QPSK signal. It is widely thought that a BER level of 10^{-5} is acceptable for a typical wireless data communication system [20]. The ideal value of E_b/N_0 to achieve this was found to be 19 dB, according to (7). Hence, with an effective bandwidth of 350 kHz, with reference to (13), the maximum data rate that could be obtained from the channel is calculated to be 1.3 Mb/s. This simulation thus represents the ideal situation, with the correct value of SNR being available, and it would be expected that the ultrasonic system would need to approach this value if it was to be useful as a short-range communication system.

A pulse-shaped QPSK signal performs better than one in which the envelope is not shaped in terms of the received signal quality, as shown in Fig. 7, when considering the EVM for a given value of E_b/N_0. This is because the required signal bandwidth to accommodate the pulse can be less than for the unshaped case, thereby reducing the noise bandwidth correspondingly. The comparison is made for a channel simulation in which AWGN was used for the noise model. In this simulation, the E_b/N_0 ratio was incremented in 3-dB steps from 16 to 40 dB.

For an example of this improvement, using a bit-rate of 200 kb/s and a roll-off factor (α) of 0.2, the required bandwidth to pass the signal was reduced from 200 to 120 kHz. This corresponded to a lower EVM for the pulse-shaped approach for values of E_b/N_0 up to 28 dB. For higher values of E_b/N_0, and when filtering with values of α greater than 0.2, the EVM became slightly larger. Under higher E_b/N_0 values and for the greater values of α, the bandwidth effective occupancy was better and the phase transitions were smoother, leading to improved ISI.

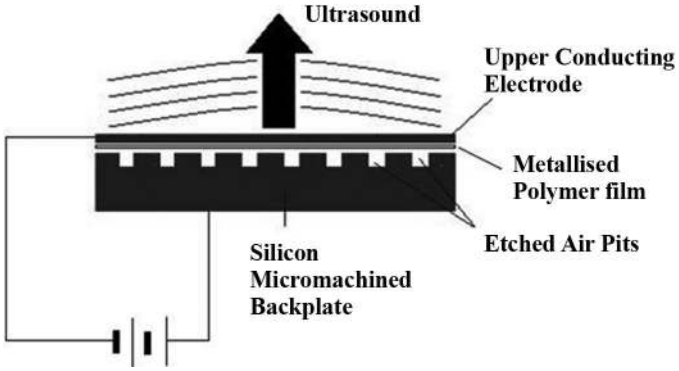

Fig. 4. Schematic diagram of an air coupled micromachined capacitive transducer.

Fig. 8 shows the result of applying RC filtering on square pulses with a roll-off factor of 0.2, which is the output from a bit splitter (see Fig. 1). According to the left side of Fig. 8, the RC-filtered pulses no longer have constant amplitude but the phase transition has been smoothed. It is evident from the right side of Fig. 8 that the sidelobes have been almost eliminated, thus reducing the ISI. Also, the effective bandwidth of the RC-filtered baseband signal has been reduced from 100 to 60 kHz. It is therefore concluded that pulse shaping has benefit in terms of both bandwidth efficiency and power efficiency.

For the simulations that follow, the baseband signal was chosen to be a 180-bit binary stream, as shown in Fig. 1. The bit rate R_b was 200 kb/s, and the duration of the signal was 0.9 ms. The sampling frequency f_s was chosen to be 2 MHz, i.e., 20 samples per symbol. The noise in the channel was assumed to be AWGN, and independent of the signal. Hence, the degradation of the received signal quality is mainly caused by scattering and absorption.

The results from simulations of a QPSK scheme are shown in Fig. 9, using the experimental characteristics shown earlier in Fig. 6. Values of $\alpha = 0.2$ and B = 120 kHz were used. Results are shown both for an ideal case (no noise), and with noise added to simulate an actual experiment, resulting in an SNR for the received waveform of 20 dB. It can be seen that the signal spectrum is still visible even with the addition of noise. The dashed line indicates the measured channel response at a distance of 1.2 m.

This is illustrated in more detail by the constellation diagrams, for both transmitted and received signals, in Fig. 10. As expected, the received signal demonstrates greater scatter, and a higher EVM value, than originally transmitted. The corresponding eye diagrams for these simulations are shown in Fig. 11. Filtering by the channel

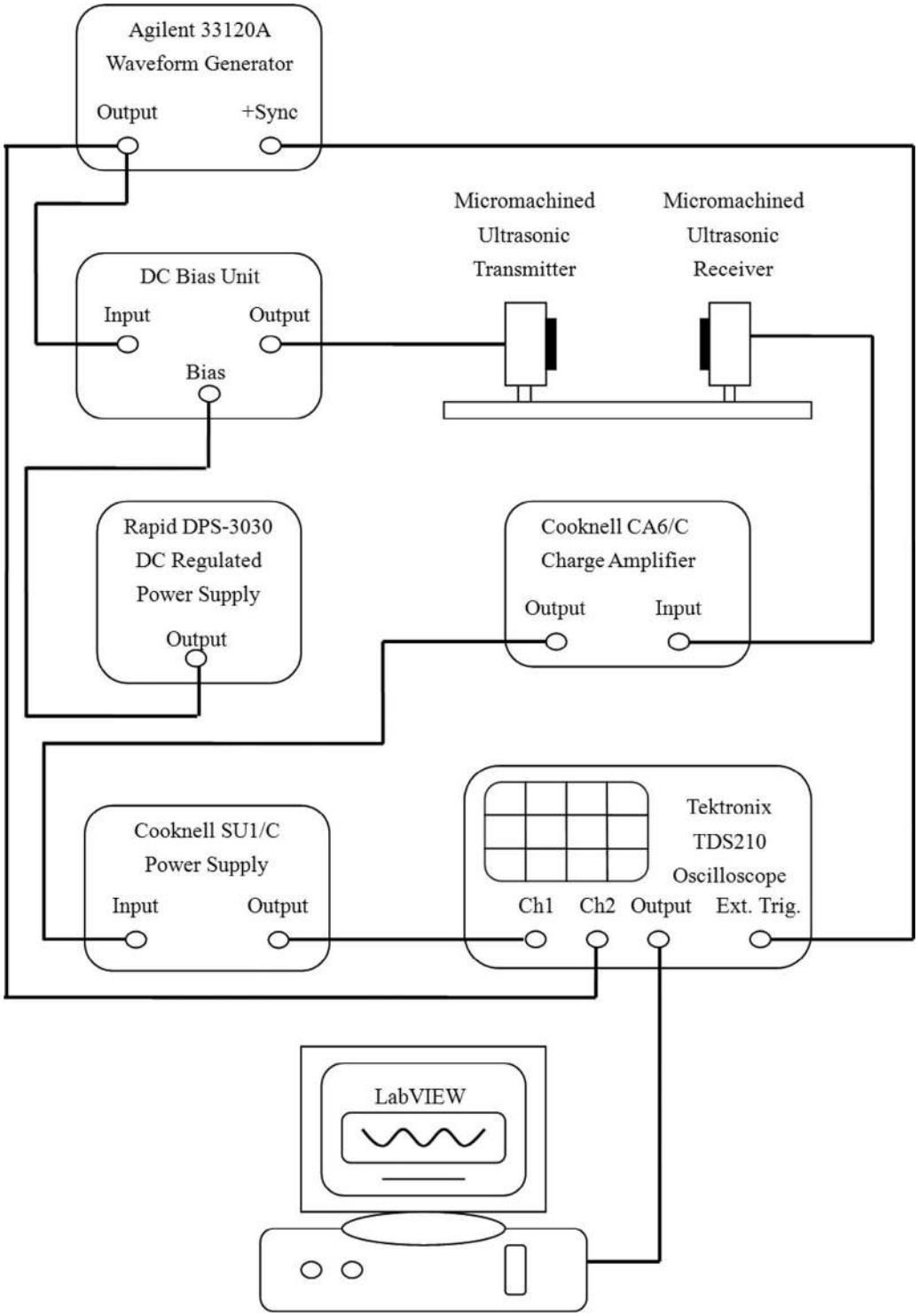

Fig. 5. Schematic diagram of the experimental arrangement.

response and adding white noise has caused the vertical extent of the central "eye" to be reduced for both channels (an indication of such factors—a more open eye is better). The eye is also wider. This means that data can be sampled over a more extended time duration, which is also a benefit. Also, on the transmitted signal, distinct traces which cross the horizontal axis are seen, whereas in the simulated received signal these are less distinct—an indication of the presence of noise.

V. Results and Discussion

The above simulations indicated that ultrasonic communications based on QPSK signals would be feasible across a distance in excess of 1 m in air. Experiments were thus performed to confirm that this was the case, and to indicate how the performance was modified by changes in factors such as the roll-off factor (α) of the filter used in the QPSK scheme.

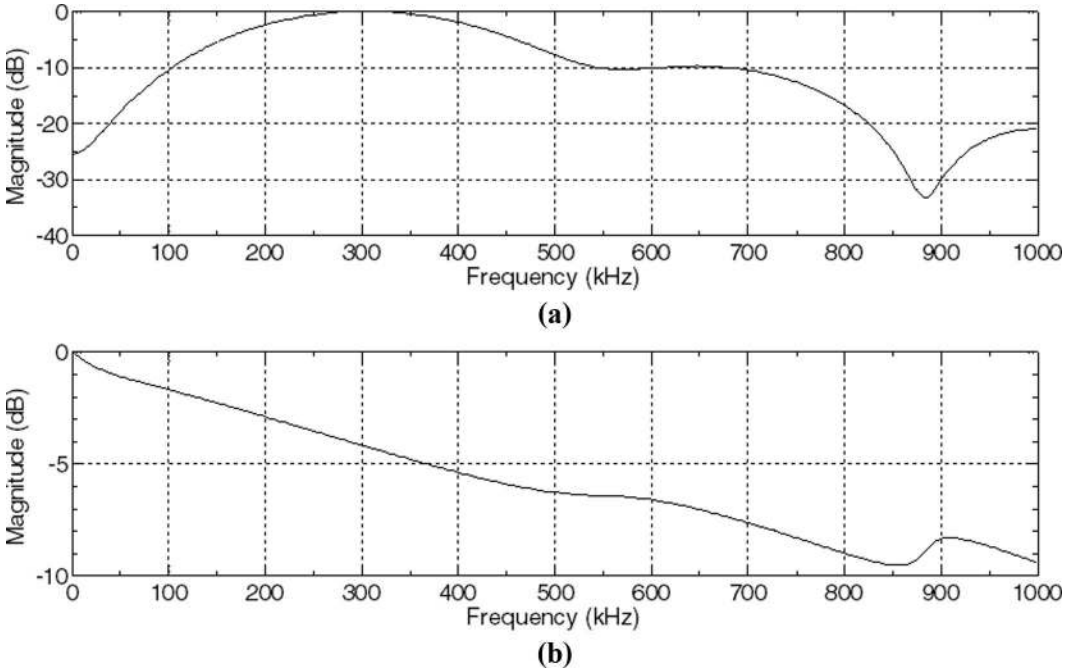

Fig. 6. (a) Magnitude and (b) phase response of the ultrasonic system as measured experimentally.

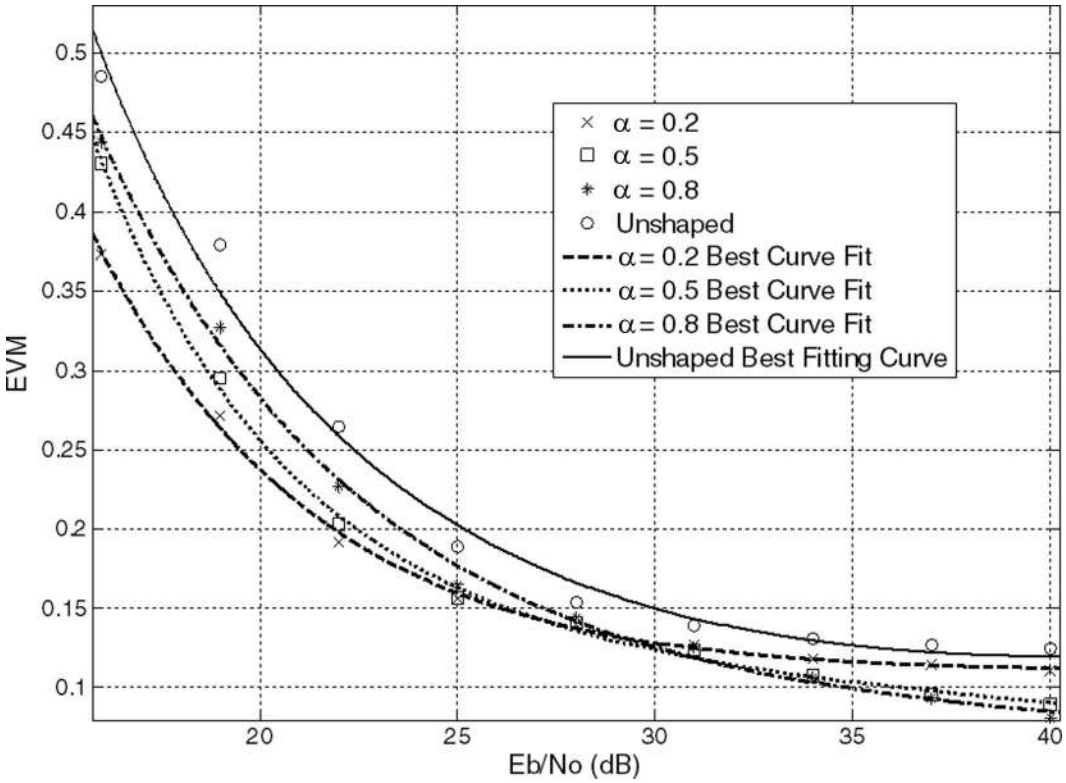

Fig. 7. Simulation results: comparison of performance with and without pulse shaping.

Fig. 12 shows the results of an experiment in air, using 2 capacitive transducers in the arrangement shown in Fig. 5. The distance between the transducers was 1.2 m, and the bandwidth used was 120 to 200 kHz. Bit rate was chosen to be 200 kb/s. Fig. 12 shows the received ultrasonic waveform for 4 values of α on the left, with the equivalent frequency spectrum on the right in each case.

From Fig. 12 it can be seen that the amplitude of the received QPSK waveform increased with an increase of the pulse-shaping roll-off factor. The received unshaped QPSK signal tended to give the strongest signal of the 4 cases; however, it occupied the widest bandwidth, and this is a disadvantage when bandwidths are limited in an ultrasonic communication system. It is also clear that in

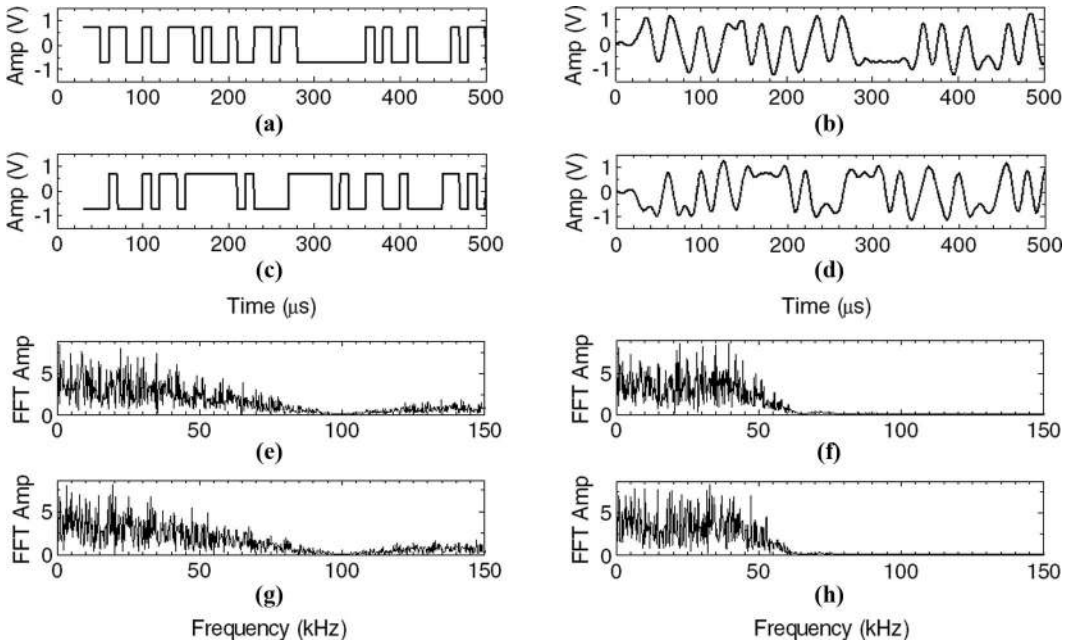

Fig. 8. (a) I-channel square pulse and (b) its spectrum; (c) I-channel raised cosine shaped pulse and (d) its spectrum; (e) Q-channel square pulse and (f) its spectrum; (g) Q-channel raised cosine shaped pulse and (h) its spectrum.

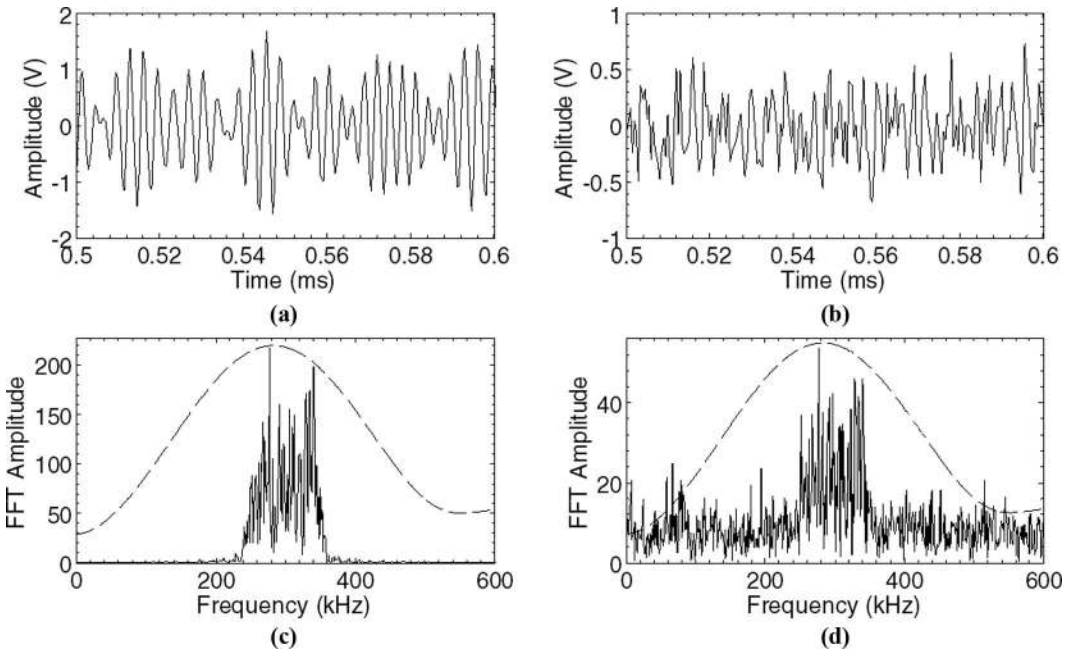

Fig. 9. Simulations of a quadrature phase shift keying ultrasonic communication system after propagation across an air gap of 1.2 m. (a) Transmitted waveform, (b) received waveform with added noise and adjusted for channel response, (c) transmitted spectrum, and (d) spectrum of simulated received signal.

all 4 spectra, transmitted signals have been filtered by the channel magnitude response, which includes the response of the frequency selective attenuation in air while propagating over a relatively long range, such that the higher frequencies are attenuated more than the lower frequencies.

Using the transmitted QPSK as a reference, the experimental performance in terms of MER and EVM defined earlier can be evaluated. Discrete experimental results are presented, together with a best fitting curve to the data in Fig. 13, for various values of α. Note that it has been found experimentally that errors start to appear in decoding when the value of EVM is over 0.2 (i.e., 20%); thus, while the unshaped response may appear attractive in terms of amplitude, there are other factors to be considered in a real communication system.

Fig. 13 shows that at high E_b/N_0 (over 35 dB), unshaped QPSK appears to achieve a lower value of EVM,

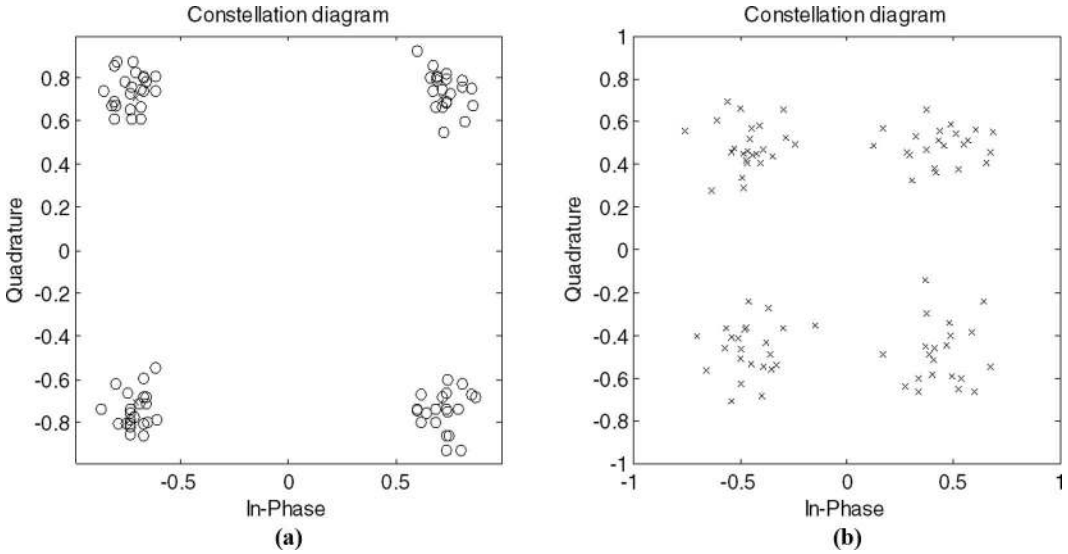

Fig. 10. Simulated quadrature phase shift keying constellation diagrams for (a) the transmitted ultrasonic signal (error vector magnitude, EVM = 9.1%) and (b) the received ultrasonic signal (EVM = 16.4%).

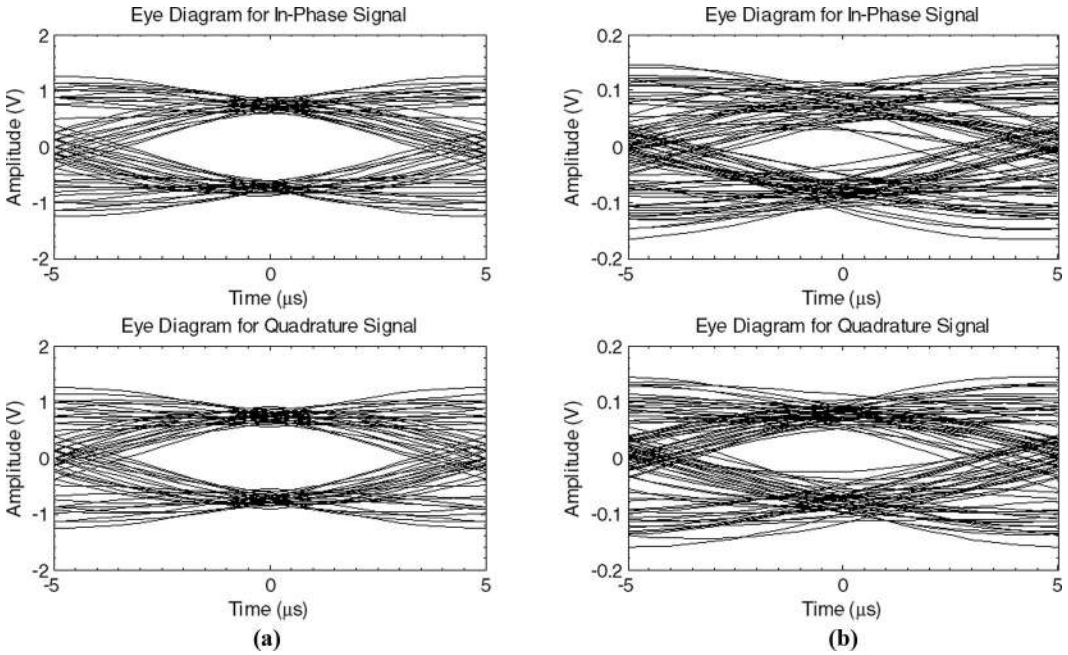

Fig. 11. Simulated quadrature phase shift keying eye diagram for both the I and Q channels in an ultrasonic communication system, for the (a) transmitted and (b) received signal.

and hence a better performance. However, at low E_b/N_0 values (less than 22 dB), a shaped QPSK becomes of more value. It is found in this experiment that an EVM value higher than 0.2 will lead to a severe BER in decoding, which could cause the transmitted information to become unusable. With $\alpha = 0.8$, a reliable communication link could be established when E_b/N_0 is greater than 20 dB. On the other hand, if bandwidth efficiency is the top priority, by setting $\alpha = 0.2$, the channel will not be sufficiently robust unless the E_b/N_0 reaches a value of 35 dB. However, with $\alpha = 0.5$, a reasonable compromise between bandwidth occupation and performance can be expected within the range 19 to 33 dB. It is also evident that the fall in experimental EVM curves is much steeper than those obtained from simulation. This is mainly caused by the frequency-selective attenuation for ultrasound propagation in air, which will be discussed and modeled in the next paper.

Figs. 14–17 show constellation and eye diagrams for 4 values of α. It can be seen that the linear phase response of the system has kept the QPSK constellation in place regardless of the unbalance of magnitude response (*i.e.* the center point of the 4 constellation groupings remains virtually the same, although the individual points can be more widely spread over the diagram). This again emphasizes the advantages of using phase modulation. The level of the opening of the eye was found to be directly

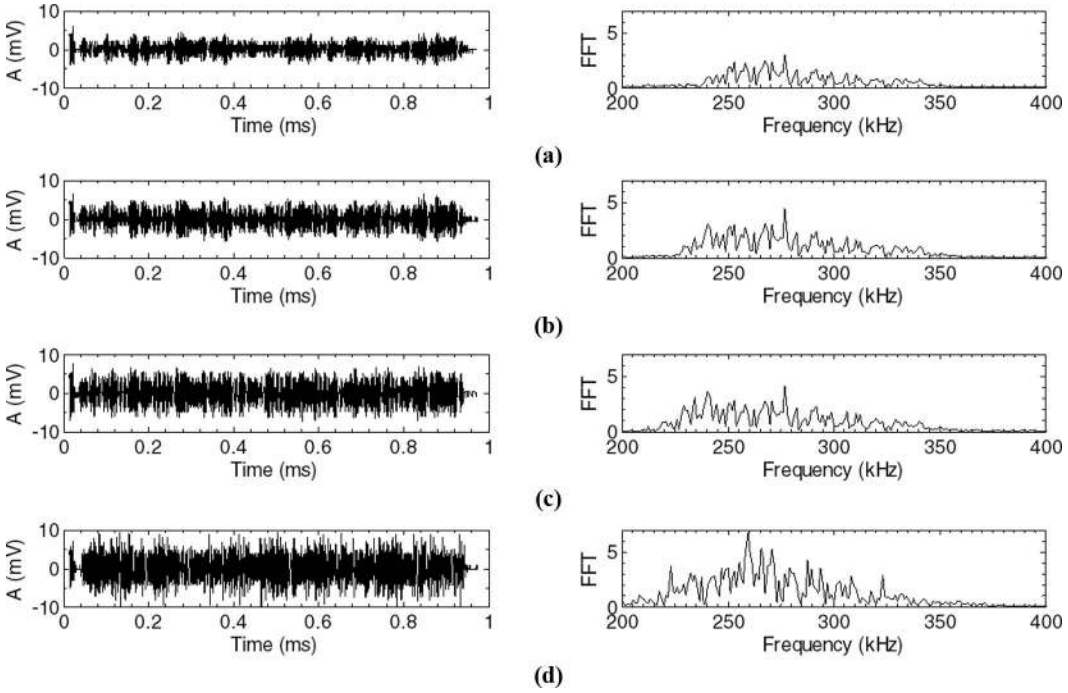

Fig. 12. Results of a quadrature phase shift keying ultrasonic transmission across air for (a) $\alpha = 0.2$, (b) $\alpha = 0.5$, (c) $\alpha = 0.8$, and (d) an unshaped experiment ($\alpha = 1$), recorded at distance of 1.2 m. In each case the time waveform is on the left, and the corresponding frequency spectrum is on the right.

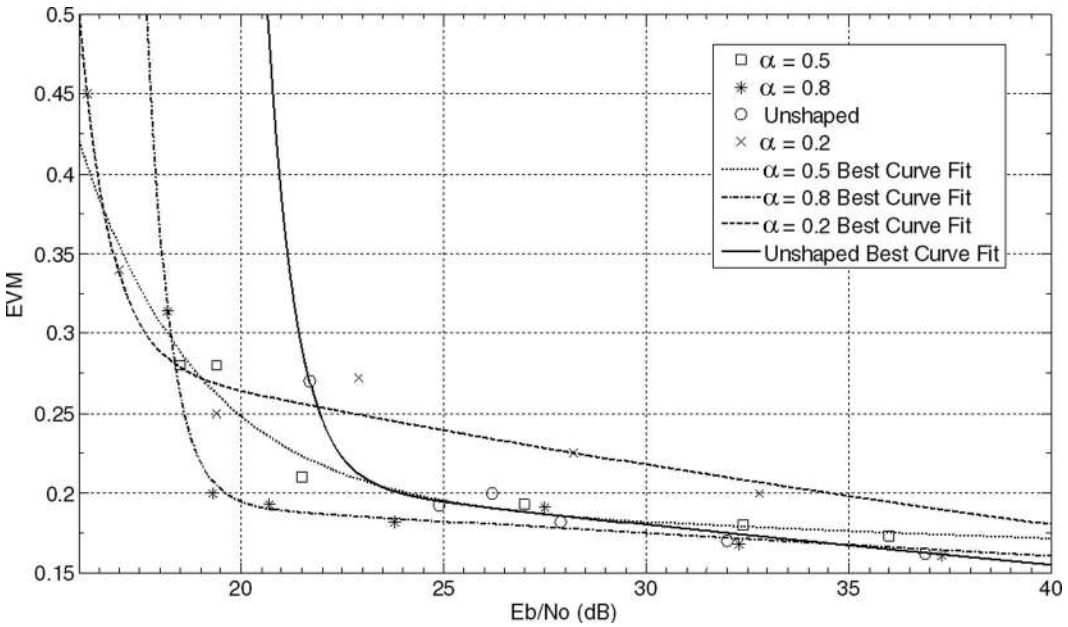

Fig. 13. Comparison of the experimental error vector magnitude that results from a given value of E_b/N_0 (discrete points) with curves predicted by theory, for various values of α.

proportional to the roll-off factor. However, the in-phase (**I**) channel and the quadrature (**Q**) channel have showed different opening characteristics of their eye diagrams. This could have been caused by the unavoidable phase synchronization error.

The more open the eye, the better the separation in the scatter plot, which also means that the SNR/MER is better. Hence, signal transmission is likely to be more robust (less susceptible to noise). The horizontal width of the eye diagram represents the time over which the signal can be successfully treated to decode the signal—i.e., the wider the eye, the better. From Figs. 14 to 17, it is evident that a wider eye has resulted from an increase in the value of α.

VI. Conclusions

The initial simulations indicated that QPSK modulation would be a good choice for ultrasonic communications

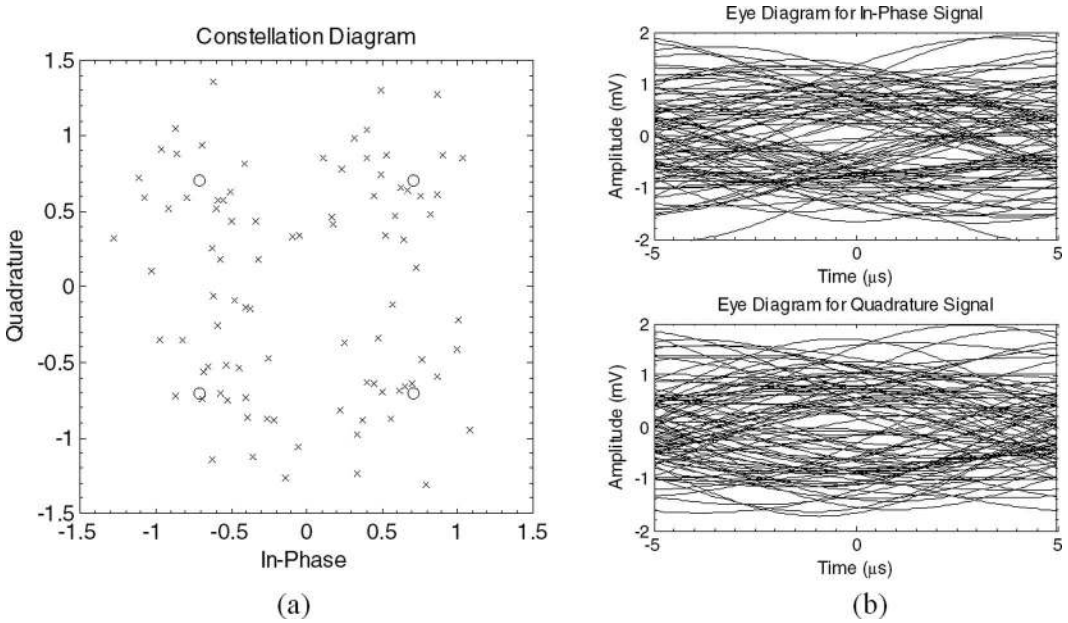

Fig. 14. (a) Constellation diagram for received quadrature phase shift keying with $\alpha = 0.2$. The crosses represent the amplitude of each channel after decoding. (b) Corresponding eye diagram.

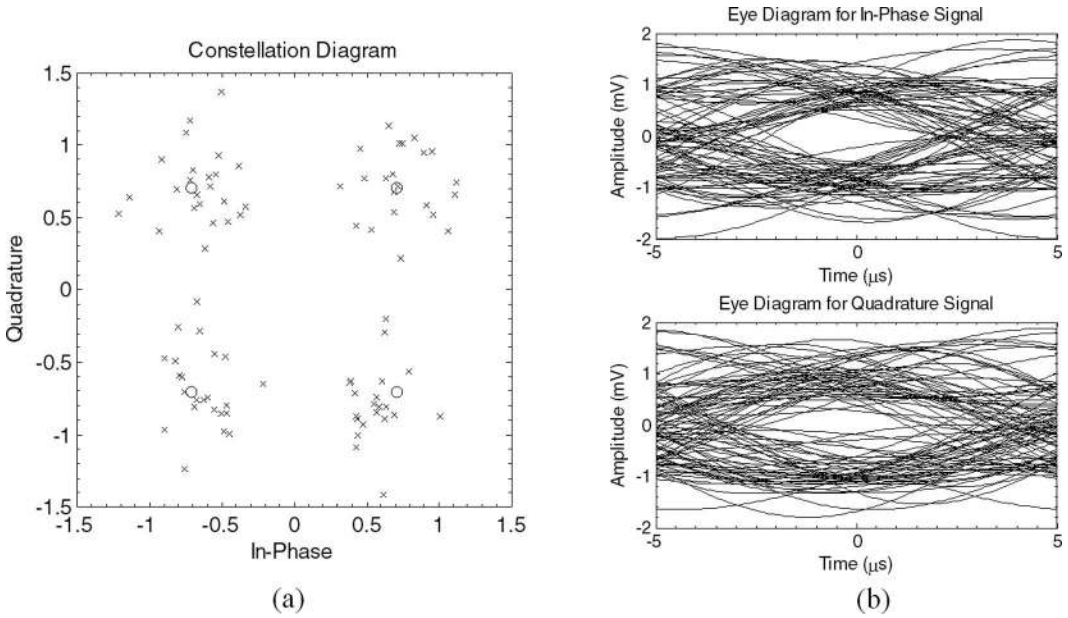

Fig. 15. (a) Constellation diagram and (b) eye diagram for received quadrature phase shift keying with $\alpha = 0.5$.

in air. Initial experiments identified the frequency response of the ultrasonic system in air in terms of amplitude and phase. This was then used to design the approximate characteristics that would be needed in a QPSK system for ultrasonic use with the transducers used. Reasonable performance in terms of EVM and E_b/N_0 was obtained in both simulations and subsequent experiments. The results have indicated that a QPSK approach can be used to propagate ultrasonic signals in air over reasonable distances in the 1 to 2 m range indoors.

The choice of filter seems to have a relatively large effect on performance. This is characterized by the value of α. In most conventional RF communication systems, α tends to be set at a value of around 0.2; this is so that multiple channels can be used over a restricted bandwidth. In the case of ultrasonic communication systems, values of α could be chosen within the range 0.2 to 0.8, subject to the available bandwidth of the channel and the maximum EVM allowed for a successful decoding.

The work in this paper was performed over relatively short distances in a laboratory environment. In practice, other factors are likely to influence performance. These include air turbulence, frequency-dependent attenuation in air, the effect of spatial response of the transducer system,

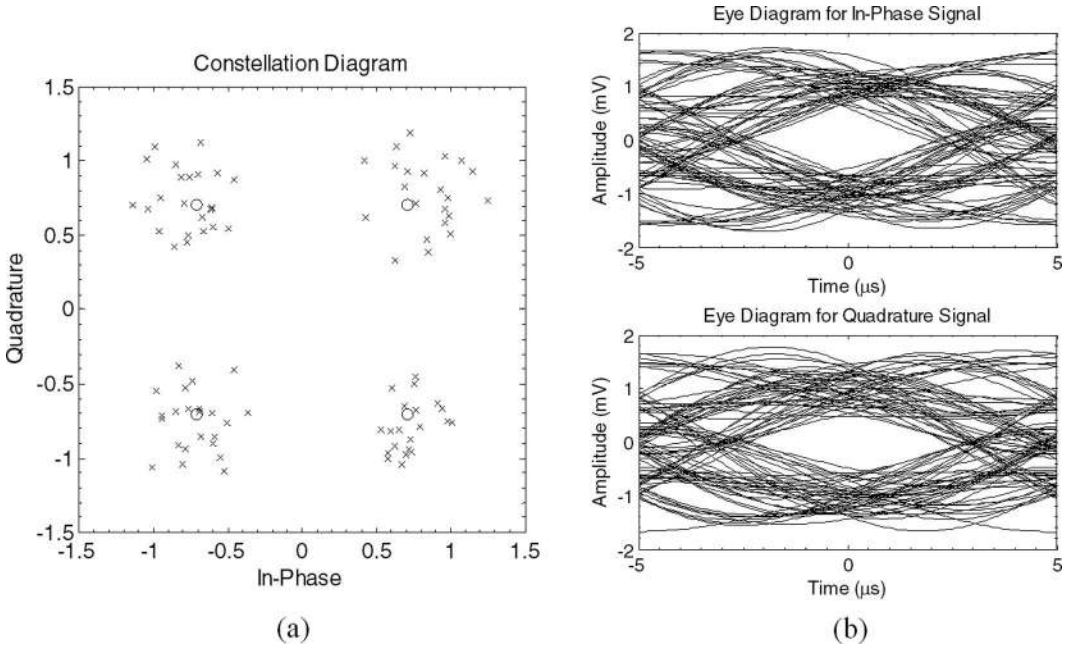

Fig. 16. (a) Constellation diagram and (b) eye diagram for received quadrature phase shift keying with $\alpha = 0.8$.

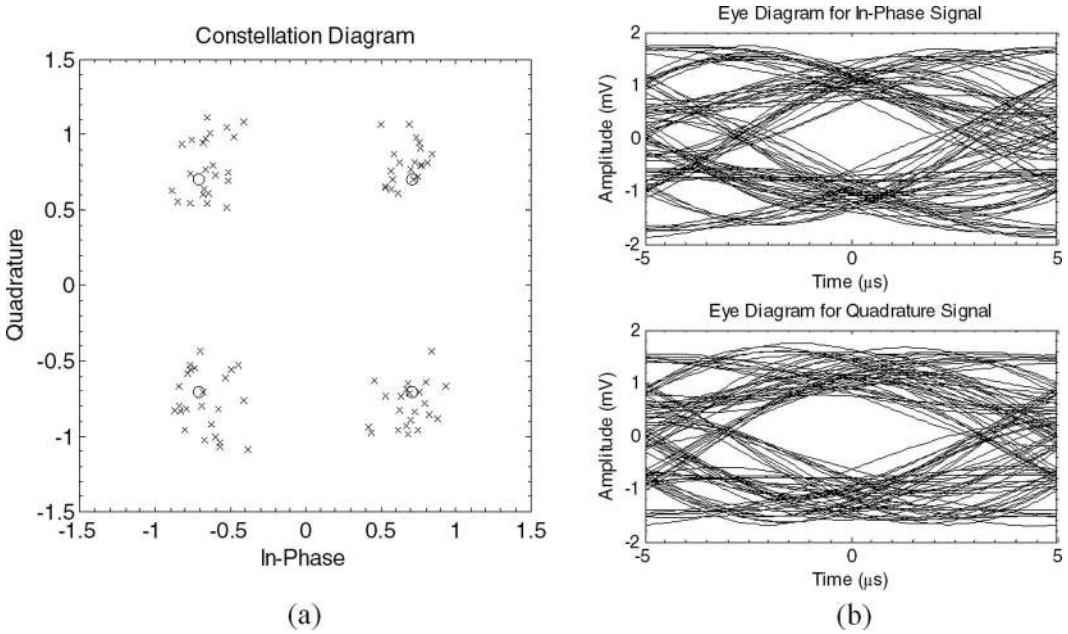

Fig. 17. (a) Constellation diagram and (b) eye diagram for received quadrature phase shift keying unshaped.

and multiple reflections (the so-called multi-path problem in communications). All these factors are currently under investigation.

References

[1] A. Bensky, *Short-Range Wireless Communication: Fundamentals of RF System Design and Application*, 2nd ed. Burlington, MA: Newnes, 2004, pp. 115–150.

[2] S. Ahson and M. Ilyas, *WiMAX: Standards and Security*. Boca Raton, FL: CRC Press, 2008, pp. 201–210.

[3] J. P. K. Gilb, "Bluetooth radio architectures," in *Radio Frequency Integrated Circuits (RFIC) Symp., Dig. Papers*. Jun. 2000, pp. 3–6.

[4] J. R. Barry, *Wireless Infrared Communications*. Boston, MA: Kluwer Academic, 1994, pp. 50–54.

[5] K. Yutaka, O. Yoshihiro, and U. Hiroshi, "International standard of infrared data communication, IrDA," *Shapu Giho/Sharp Tech. J.*, no. 68, pp. 11–17, Aug. 1997.

[6] B. Matthieu, B. Joao, M. R. D. Rodrigues, and S. W. McLaughlin, "Wireless information—Theoretic security," *IEEE Trans. Inf. Theory*, vol. 54, no. 6, pp. 2515–2534, Jun. 2008.

[7] J. Nakrop, W. Sodsai, N. Prasit, and S. Atipong, "Security system against asset theft by using radio frequency identification technology," in *5th Int.Conf. Electrical Engineering/Electronics, Computer, Telecommunications, and Information Technology*, vol. 2, May 2008, pp. 761–764.

[8] T. Tsutomu, S. Masahiro, and Y. Susumu, "Multipath delay estimation for indoor wireless communication," in *IEEE Vehicular Technology Conf.*, May 1990, pp. 401–406.

[9] A. Gachagan, G. Hayward, S. P. Kelly, and W. Galbraith, "Characterization of air-coupled transducers," *IEEE Trans. Ultrason. Ferroelectr. Freq. Control*, vol. 43, no. 4, pp. 678–689, 1996.
[10] D. M. Mills and S. W. Smith, "Multilayered PZT/polymer composites to increase signal to noise ratio and resolution for medical ultrasound transducers," *IEEE Trans. Ultrason. Ferroelectr. Freq. Control*, vol. 49, no. 7, pp. 1005–1014, Jul. 2002.
[11] C. Li, D. A. Hutchins, and R. J. Green, "Short-range ultrasonic digital communications in air," *IEEE Trans. Ultrason. Ferroelectr. Freq. Control*, vol. 55, no. 4, pp. 908–918, Apr. 2008.
[12] S. Holm, "Airborne ultrasound data communications: The core of an indoor positioning system," in *Proc. IEEE Ultrason. Symp.*, Rotterdam, The Netherlands, vol. 3, Sep. 2005, pp. 1801–1804.
[13] R. A. Zurek, M. L. Charlier, and A. Dietrich, "Omnidirectional ultrasonic communication system," U.S. Patent 6363139, Mar. 26, 2002.
[14] H. D. Haynes, M. A. Akerman, and V. M. Baylor, "Ultrasonic communication project phase 1 final report," National Security Program, Oak Ridge, TN, Office Rep. Y/NSP-252, Jun. 2000.
[15] K. Mizutani, N. Wakatsuki, and K. Mizutani, "Acoustic communication in air using differential biphase shift keying with influence of impulse response and background noise," *Jpn. J. Appl. Phys.*,vol. 46, pp. 4541–4544, Jul. 2007.
[16] H. Ochi and T. Fukuchi "Development of tilted toroidal beam wideband transducer using quadrature phase shift keying for underwater acoustic communication," *Jpn. J. Appl. Phys.*, vol. 46, pp. 4961–4967, Jul. 2007.
[17] A. Mansukhani, "Wireless digital modulation," *Appl. Microw. Wirel.*, vol. 8 no. 4, Nov.–Dec. 1996, pp. 501–504.
[18] D. W. Schindel, D. S. Forsyth, D. A. Hutchins, and A. Fahr, "Air-coupled ultrasonic NDE of bonded aluminium lap joints," *Ultrasonics*, vol. 35, no. 1, pp. 1–6, Feb. 1997.
[19] D. W. Schindel, D. A. Hutchins, L. Zou, and M. Sayer, "The design and characterization of micromachined air-coupled capacitance transducers," *IEEE Trans. Ultrason. Ferroelectr. Freq. Control*, vol. 42, no. 1, pp. 42–51, Jan. 1995.
[20] O. Hiroshi, W. Yoshitaka, and S. Takuya "Experiments on acoustic communication with quadrature amplitude modulation in multipath environment," *Jpn. J. Appl. Phys.*, vol. 43, no. 5B, pp. 3140–3145, May 2004.

Chuan Li received the B.Eng. and M.Sc. degrees in electronic engineering from the University of Warwick, UK, in 2004 and 2006, respectively. He is currently doing full-time Ph.D. research in ultrasonic communications at the same institution. In recent years, his research interests have included ultrasonic communications using electrostatic transducers and infrared communications.

David Hutchins obtained his B.Sc. and Ph.D. degrees from the University of Aston, Birmingham, UK. After holding several postdoctoral positions, he joined the faculty of Queen's University, Ontario, Canada. He then moved to the University of Warwick, UK, where he is currently a professor in the School of Engineering. His research interests include noncontact ultrasound, micromachined transducers, ultrasonic imaging, and nondestructive evaluation.

Roger J. Green (M'86–SM'88) became professor of electronic communication systems at the University of Warwick in September 1999, and head of the Division of Electrical and Electronic Engineering in August 2003. He has published widely in the field of communications and has several patents. He is also a senior member of the IEEE and currently serves on two IEEE committees concerned with communications and signal processing.